

## Numerical Investigation of the Effect of Design Parameters on the Blade Flutter Prediction

F. A. Abdukhakimov<sup>a,\*</sup>, V. V. Vedeneev<sup>a</sup>, M. E. Kolotnikov<sup>a</sup>, and P. V. Makarov<sup>b,\*\*</sup>

<sup>a</sup> *Lomonosov Moscow State University, Moscow, 119991 Russia*

<sup>b</sup> *“Salut” Gas Turbine Engineering Research and Production Center, Moscow, 105118 Russia*

\**e-mail: farruh.abduhakimov7@gmail.com*

\*\**e-mail: makarovpv@yandex.ru*

Received June 25, 2017; revised April 13, 2018; accepted December 24, 2018

**Abstract**—Blade flutter is one of the major problems that designers of modern gas-turbine engines face. As a rule, the flutter of compressor blades is predicted using simplified criteria devised in design organizations based on the experience of designing and refining engines. In this paper a study of the influence of the design parameters on prediction of blade flutter in compressors of gas-turbine engines is presented. Empirical and probabilistic criteria are not applicable to evaluation of the flutter since the parameters in question are not among the decisive parameters for simplified criteria. In this work, a numerical algorithm for prediction of the flutter based on the energy method is used. The algorithm is applicable if the oscillation modes in vacuum are close to the corresponding modes in a flow, a condition that is always met for compressor blades, with the exception of rarely used hollow blades and blades of composite materials. It is shown that the inter-blade tension has a significant influence on the flutter boundaries, while the effect of other design parameters under investigation on the flutter boundaries is insignificant.

**Keywords:** blade flutter, energy method, compressor, gas-turbine engine.

**DOI:** 10.3103/S105261881902002X

Developers of gas-turbine engines were faced with the phenomenon of compressor blade flutter in the mid-1950s when developing second-generation engines. Vast practical experience of studying flutter has been gained [1]. However, until now, there has been no generally accepted method for prediction of the compressor blades within a wide range of operating conditions, which is especially important at the design stage. When designing engines, engineers and designers use, as a rule, simplified criteria, viz., the Strouhal number, bending–torsion coupling, etc., based on the experience gained from design organizations in designing and refining engines. The statistical method [2] based on the processing of a great number of tests and the prediction of the blade flutter of new compressors yields results that are more precise.

Another method for prediction of the blade flutter is the frequency-response method based on calculation of natural frequencies of a coupled flow–blade system. Under this approach, the positivity of the imaginary components of the natural frequency is a criterion of the flutter onset. However, the associated problem of finding complex eigenvalues of nonsymmetric matrices requires great computational resources. The frequency-response method and its variations are used in [3–7]. The problem of predicting the flutter is also dealt with in [8, 9] where a direct method is used; the essence of the method is the modeling of the movement over time of a coupled blade–flow system. The numerical calculations, however, require considerable computational resources. In [10, 11], an energy method is used; the method is based on calculation of the work performed by aerodynamic forces on the surface of a blade that oscillates harmonically in its natural mode over an oscillation period.

In this paper, the effect of the design parameters, viz., the radial clearance, the closing and opening angles of the inlet guide vanes, the radial flow nonuniformity, and the magnitude of the inter-blade tension in the mid-span shroud, on the results of the blade flutter prediction is studied numerically. Simplified criteria are not applicable to evaluation of the effect of the above factors on flutter prediction since the design parameters do not play a decisive role in such criteria.

To predict the flutter, a previously developed numerical algorithm based on the energy method [12, 13] was used in the investigations. The applicability of the algorithm is limited by the unstall airflow condition

in the interblade passage, which is characteristic of the compressor's operating conditions. In [12, 13], the convergence is investigated and the parameters of numerical modeling are provided that assure correct performance of calculations. The results obtained were verified by the results of full-scale tests of a compressor.

**The flutter prediction method.** We assume that the influence of the airflow on the blades' natural oscillations is insignificant. Then, the airflow may cause only additional damping—in the case of stability—or strengthening—in the case of flutter—of oscillations without changing the natural modes and frequencies compared with oscillations in a vacuum. The equation of energy for a blade in the system of rotating coordinates coupled with the wheel has the form

$$\frac{dE(t)}{dt} = A(t),$$

where  $E(t)$  is the total energy and  $A(t)$  is the power of internal and external forces. As a conservative estimate, we neglect the structural damping considering only the pressure distributed over the blade surface. Then, the change in the total energy over one oscillation period has the form

$$\Delta E = W = \int_{t_0}^{t_0+T} \int_S p(x, y, z, t) \mathbf{n}(x, y, z, t) \mathbf{v}(x, y, z, t) ds dt,$$

where  $T = 1/f$  is the oscillation period of the blade,  $f$  is the natural frequency,  $S$  is the blade surface,  $p$  is the pressure,  $\mathbf{n}$  is the normal to the blade surface, and  $\mathbf{v}$  is the velocity of the blade points. We neglect the viscous stresses in the air, as they do not usually influence the flutter boundaries.

Since the impact of the flow on the oscillations of the blades is weak, calculated work  $W$  is also low. The work done over harmonic oscillations (at a constant amplitude) differs from the actual work at an increasing or decaying oscillation by the value of the second order of infinitesimals, which is negligible. The mode and frequency of the harmonic oscillations are calculated for a blade in a vacuum using a standard engineering software tool.

In this way, the work done by the unsteady pressure over the oscillating blade over one oscillation period is calculated. If the work is positive, in each period of oscillation, the energy is boosted from the flow to the blade and its amplitude is increased. If the work is negative, in each period of oscillation, part of the energy of the blade is dissipated in the flow. As a consequence, the following inequality

$$W > 0 \quad (1)$$

serves as the flutter criterion.

From the point of view of its geometry, the gas flow model consists of three successive blade passages of one wheel (Fig. 1a). To calculate the transient airflow, the initial and boundary conditions are set from the stationary flow calculated for the whole compressor, i.e., all stages are modeled, and verified by full-scale field tests of the compressor integrated into the engine. The distribution of the total pressure, the total temperature, the directions of the velocity vector and turbulence parameters at the inlet in the blade passage, and the distribution of the static pressure at the outlet from the impeller passage are specified as the boundary conditions. On the surfaces of solid bodies such as the hub, blades, and casing, the no-slip conditions are set. On the outer side boundaries of the model, the cyclic symmetry condition is assumed (Fig. 1b).

On the surface of every blade, the displacement of the computational domain boundary is prescribed in the form of the natural oscillation of the wheel (traveling wave) with a preset number of nodal diameters as

$$\mathbf{u}(x, y, z, t) = A(\sin \omega t \cdot \mathbf{L}_1(x, z) - \cos \omega t \cdot \mathbf{L}_2(x, z)),$$

where  $A$  and  $\omega = 2\pi f$  are the amplitude and circular frequency of the oscillating blade and  $\mathbf{L}_1(x, z)$  and  $\mathbf{L}_2(x, z)$  are the functions that interpolate the natural oscillation modes that correspond to the node and antinode of the disk–blades–shroud system. To interpolate the calculated results of the modal analysis and transport them to the CFD code, tenth-degree Lagrange polynomials are used [12, 13]. According to the preset boundary displacement, the aerodynamic computational grid of the blade airfoil is distorted. To model a wave that travels forward or backward over the impeller, which is characteristic of the cascade flutter [1, 14], phase lag  $\sin \omega t - \varphi$  or phase lead  $\sin \omega t + \varphi$  with respect to the central blade, where phase shift  $\varphi = 2\pi m/N$  is determined by the number of the nodal diameters  $m$  ( $N$  is the number of the blades in a stage), is preset on the side blades.

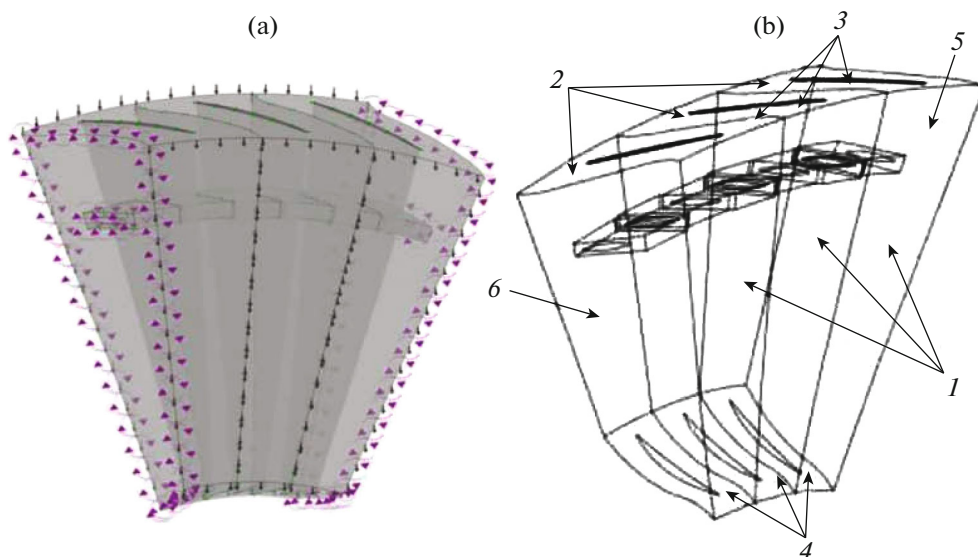


**Fig. 1.** (a) Computational aerodynamic model and (b) boundary conditions: (1) inlet, (2) outlet, (3) casing, (4) hub, and (5, 6) outer side boundaries.

According to the above procedure, flutter is predicted in four stages.

(1) Calculation of the natural frequencies and modes of the elastic disk–blades–shroud system in a vacuum. Interpolation of the oscillation modes of the blade airfoil by Lagrange polynomials.

(2) Calculation of the steady-state airflow in the compressor.

(3) Transient calculation of the flow in a selected stage with blades that oscillate in its natural mode calculated in step 1, i.e., with the preset displacement of the aerodynamic computational grid of the blade foil.

(4) Calculation of the work done by the pressure over the central blade and verification of flutter criterion (1).

Steps 3 and 4 are performed for every natural mode potentially prone to flutter at several nodal diameters for forward- and backward-travelling deformation waves. These modes are the first and second flexural modes and the first torsional mode [1]. The work is calculated for the last of several calculated oscillation periods so that the response of the pressure to harmonic oscillations of the blade also becomes harmonic. The calculations show that three oscillations period suffice [12, 13].

To calculate the airflow, the Ansys CFX 15.0 software for finite volume analysis is used. The Reynolds averaged Navier–Stokes equations with the  $k - \omega$  turbulence model are solved. To construct Lagrange polynomials and calculate the work of unsteady aerodynamic forces, a proprietary software code [12, 13] is used.

**The model under investigation.** The influence of the design parameters on the prediction of flutter was investigated in this work for the first-stage wheel of a low-pressure compressor (LPC) of a two-shaft gas-turbine engine in operation. A wheel with shrouded blades was considered.

Calculations were made on two regimes when, during the tests of the engine in the thermal pressure chamber, flutter was diagnosed or its absence was recorded. The conditions under which the calculations were made are presented in Table 1.

The effect of different design and aerodynamic parameters on the calculated results was investigated. Accordingly, the following configurations of the computational aerodynamic model were studied: the radial clearance between the blade and the casing of 0.5 mm; the radial clearance of 0.5 mm and the inlet guide vanes closed by  $1.5^\circ$ ; the radial clearance of 0.5 mm and the inlet guide vanes opened by  $2^\circ$ ; the radial clearance increased up to 1 mm; the radial clearance of 0.5 mm; and consideration of the radial nonuniformity at the engine intake (Table 2).

The blade shrouds were reproduced in the aerodynamic models of all configurations. Further, different inter-blade tension values in the mid-span shroud that affect the oscillation modes and frequencies of the blades were considered.

**Table 1.** Experimental parameters of the regimes of the low-pressure compressor of a two-shaft gas-turbine engine

Parameter	Regime 1, flutter	Regime 2, no flutter
Temperature at the engine intake, $T_{in}$ (K)	423.4	383.9
Pressure at the engine intake, $P_{in}^*$ (atm)	2.6	1.6
Airflow rate at the engine intake, $G_{a\_red}$ (kg/s)	73.27	73.59
Pressure ratio of the LPC, $\pi_c$	2	2.235
Reduced (with respect to the temperature at the engine intake) LPC speed, $n_{1red}$ (%)	76.08	75.03
Physical LPC speed, $n_{1ph}$ (%)	92.09	86.6

**Table 2.** Dependence of the pressure on the radius at the engine intake

Radius, m	Pressure, Pa	
	Regime 1	Regime 2
0.133	152457	56106
0.139	151623	55464
0.152	148387	52975
0.165	145819	51000
0.178	143957	49565
0.191	142613	48523
0.204	141607	47740
0.217	140822	47124
0.229	140190	46620
0.242	139672	46201
0.255	139240	45846
0.268	138881	45542
0.281	138581	45283
0.294	138332	45061
0.307	138127	44872
0.32	137961	44712
0.333	137829	44578
0.346	137727	44468
0.359	137649	44378
0.372	137590	44305
0.384	137550	44249
0.397	137530	44214
0.41	137512	44181
0.423	137504	44158
0.436	137508	44148
0.449	137532	44155
0.462	137575	44178

**Computational grids.** The finite element model for calculation of natural modes and frequencies of the blades consists of ~29 000 second-order-accurate solid elements, primarily, hexahedrons. The size of the grid for the aerodynamic analysis for one blade passage is about 850 000 control volumes. For resolution of the turbulent boundary layer, a grid clustering is constructed near the solid walls so that in all computations the value of  $y^+$  lies within the range 5–282 for most of the solid walls.

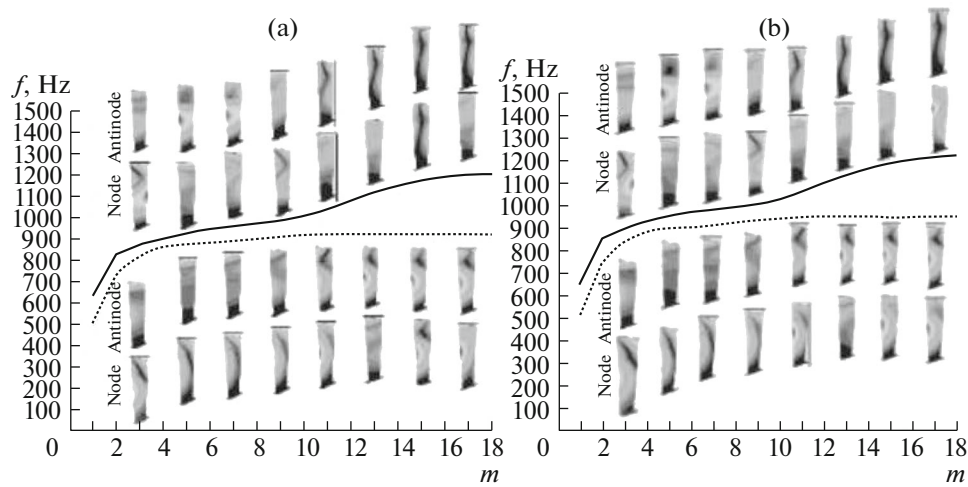


**Fig. 2.** Interference diagram for the (dashed line) second- and (solid line) third-family oscillation modes: (a) design conditions 1 and (b) design conditions 2. Shaded spots show the distribution of the displacements of the blade airfoil at the node and antinode of the disk–blades–shroud system.

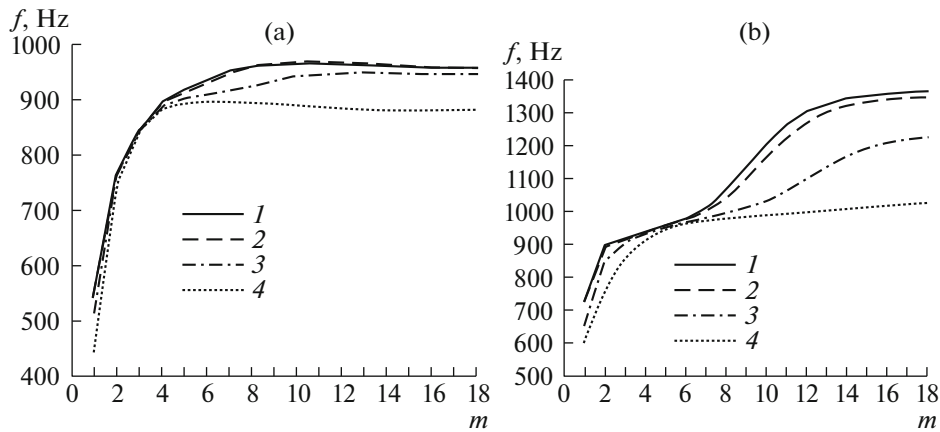


**Fig. 3.** Dispersion diagram at different inter-blade tension values under regime 1: (curve 1, solid line) 0 (no tension); (curve 2, dashed line) 0.27 mm; (curve 3, dash-dotted line) 0.54 mm; and (curve 4, dotted line) 0.8 mm. (a) The second-family oscillation modes and (b) the third-family oscillation modes.

**Calculation of natural frequencies.** The natural oscillation frequencies and modes of the disk–blades–platform–couplings system were calculated for two design conditions. For each mode, the entire range of the number of nodal diameters was investigated. The calculations accounted for the inter-blade tension caused by the overlapping of the shrouds of unstrained blades by 0.54 mm (the average value according to the drawing).

In Fig. 2, interference diagrams—the dependence of natural oscillation frequency  $f$  on the number of nodal diameters  $m$ —are shown for regime 1 and regime 2, respectively. The second and third families of the oscillation modes of the disk–blades–shroud system induced by the interference of the modes and the proneness of the latter to flutter [2] are considered.

To investigate the effect of the inter-blade tension on the flutter boundaries, the natural oscillation frequencies and modes were calculated at different inter-blade tension values for regime 1. In the interference diagram constructed for the second and third family at different interference fit values, one can see that, for the second and third modes, a decrease in the natural frequencies is observed with increasing inter-blade tension. We should note that the frequencies of the second oscillation mode family are practically indiscernible (Fig. 3) in the absence of tension and at an inter-blade tension caused by the overlapping of the blades by 0.27 mm, which is the minimum value in the drawing

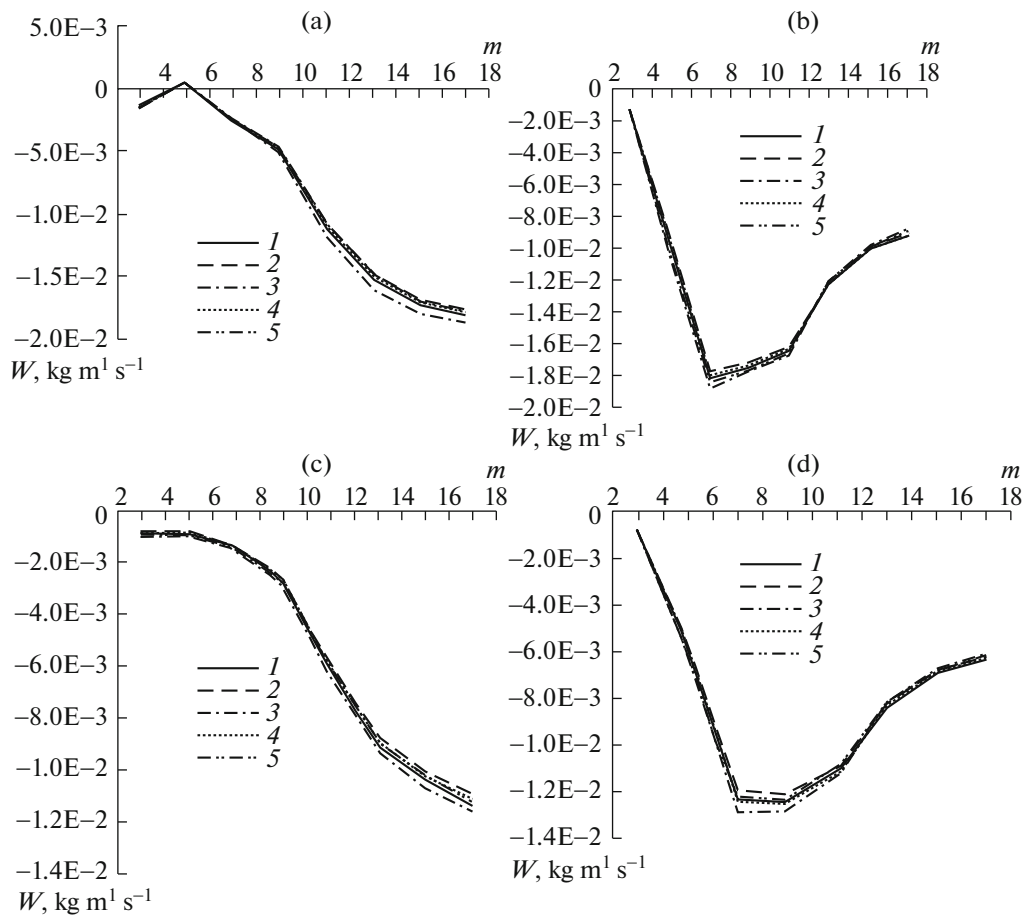


**Fig. 4.** Dependence of the pressure work on the number of nodal diameters. Regime 1. The number of the curve corresponds to the number of the configuration. (a) Regime 1, the second-family oscillation modes; (b) regime 1, the third-family oscillation modes; (c) regime 2, the second-family oscillation modes; and (d) regime 2, the third-family oscillation modes.

**Flutter calculation results.** For the second and third natural families of the oscillation modes of the shrouded first-stage wheel of the low-pressure compressor, the work of the pressure forces was calculated for various design parameters. For every natural oscillation mode family, the full range of the number of the nodal diameters was considered. The oscillation amplitude was specified in all calculations so that the maximum displacement in the blade is 0.001 m. The inter-blade tension equaled 0.54 mm in the main series of calculations.

In the curve of the dependence of the work done by the pressure forces on the number of nodal diameters for the second and third oscillation mode families for regime 1 at different configurations (see Fig. 4a), one can see that flutter is observed in all models at the second-family oscillation modes at  $m = 5$ . At other values of the nodal diameters at the second-family oscillation modes, the work of the pressure forces is negative. At the third-family oscillation modes, the work is negative with all nodal diameters.

Under regime 2, the work of the pressure forces proved to be negative (see Fig. 4b) at the second- and third-family modes in all configurations, which is consistent with the aeroelastic stability of the blades.

The data provided show that the calculated results differ insignificantly at different design and aerodynamic parameters. Consequently, the effect of the above factors on the blade flutter boundaries is not substantial.

A special series of calculations was conducted to establish the influence of the inter-blade tension in the mid-span shroud that had a considerable effect in another series of calculations [12, 13]. The results calculated for regime 1 were compared in the absence of tension and at inter-blade tension values of 0.27, 0.54, and 0.8 mm (Fig. 5). The results showed that, at the second-family modes, the work done by pressure forces was negative with all nodal diameters in the absence of the tension and at inter-blade tension

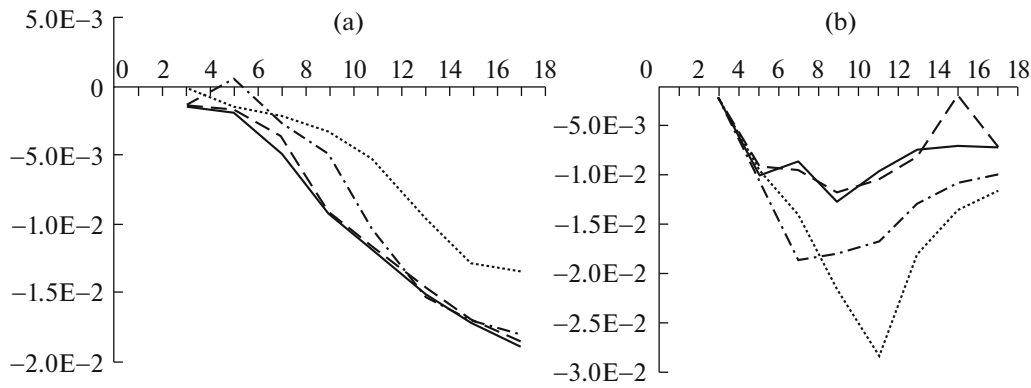


**Fig. 5.** Dependence of the pressure work on the number of nodal diameters at different inter-blade tension values. The model reproduces the shroud platforms and a radial clearance of 0.5 mm. (Curve 1, solid line) no inter-blade tension; (curve 2, dashed line) an inter-blade tension of 0.27 mm; (curve 3, dash-dotted line) an inter-blade tension of 0.54 mm; and (curve 4, dotted line) an inter-blade tension of 0.8 mm.

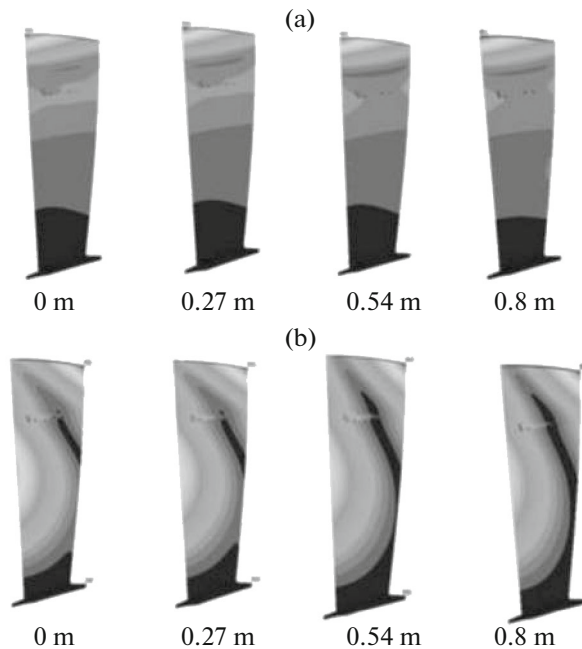


**Fig. 6.** Distribution of the displacements in the blade airfoil for the second-family modes of the oscillations of the disk-blades-shroud system that correspond to the antinode and node of the disk at inter-blade tension values;  $m = 5$ . (a) Antinode and (b) node.

of 0.27 and 0.8 mm in contrast to the results calculated at an inter-blade tension of 0.54 mm. A slight change in the oscillation modes (Fig. 6) and frequencies (Fig. 3a) at  $m = 5$  results in a change of the work sign. For the third-family oscillation modes, the work of the pressure forces is negative in all calculations. The work value at each nodal diameter differs greatly at different inter-blade tension values. It should be noted that in the absence of tension and at an inter-blade tension caused by the overlapping of the blades by 0.27 mm, the results are close at practically all nodal diameters. This is accounted for by the closeness of the natural modes and frequencies. Consequently, the inter-blade tension value influences flutter prediction to a significant degree.

In the course of this study, calculations were conducted to predict the flutter of the blades of the first-stage whell of a low-pressure compressor at various design and aerodynamic parameters of the stage. For each configuration, the dependence of the pressure work on the number of nodal diameters was obtained for the second- and third-family modes of the oscillations of the disk-blades-shroud system.

It was shown that the calculated results for the parameters in question, viz., the radial clearance magnitude, the closing and opening angles of the inlet guide vanes, and the radial flow nonuniformity, differed insignificantly within the range of changes under investigation. The above parameters almost did not affect the flutter boundary. However, the inter-blade tension had a considerable effect on the flutter calculation results owing to the change in the oscillation modes of the blades.

The results of this paper can be applied to calculations of the flutter of the blades of gas-turbine engines and gas and steam turbines and to develop efficient methods of flutter suppression.

## REFERENCES

1. Marshall, J.G. and Imregun, M.A., Review of aeroelasticity methods with emphasis on turbomachinery applications, *J. Fluids Struct.*, 1996, vol. 10, pp. 237–267.
2. Khorikov, A.A., Forecasting and diagnostics of the flutter of blades of axial compressors for aviation gas turbine engines, *Tr. TsIAM*, 2002, no. 1311.
3. Bendiksen, O.O. and Friedmann, P.P., The effect of bending-torsion coupling on fan and compressor blade flutter, *J. Eng. Power*, 1982, vol. 104, pp. 617–623.
4. Srinivasan, A.V. and Fabunmi, J.A., Cascade flutter analysis of cantilevered blades, *ASME J. Eng. Gas Turbines Power*, 1984, vol. 106, pp. 34–43.
5. Kielb, R.E. and Kaza, K.R.V., Flutter of swept fan blades, *ASME J. Turbomach.*, 1985, vol. 107, pp. 395–398.
6. Bendiksen, O.O., Role of shocks in transonic/supersonic compressor rotor flutter, *AIAA J.*, 1986, vol. 24, pp. 1179–1186.
7. Kielb, R.E. and Ramsey, J.K., Flutter of a fan blade in supersonic axial flow, *ASME J. Turbomach.*, 1989, vol. 111, pp. 462–467.
8. Bakhle, M.A., Reddy, T.S.R., and Keith, T.G., Time domain flutter analysis of cascades using a full-potential solver, *AIAA J.*, 1992, vol. 30, pp. 163–170.
9. Gnesin, V. and Rzakowski, R., A coupled fluid-structure analysis for 3-d inviscid flutter of IV standard configuration, *J. Sound Vibr.*, 2002, vol. 251, pp. 315–327.
10. Carta, F.O., Coupled blade-disc-shroud flutter instabilities in turbojet engine rotors, *ASME J. Eng. Power*, 1967, vol. 89, pp. 419–426.
11. Mikolajczak, A.A., Arnoldi, R.A., Snyder, L.E., and Stargardter, H., Advances in fan and compressor blade flutter analysis and predictions, *AIAA J. Aircraft*, 1975, vol. 12, pp. 325–332.
12. Vedeneev, V.V., Kolotnikov, M.E., Makarov, P.V., and Firsanov, V.V., Three-dimensional modeling of the flutter of compressor blades of modern GTE, *Vestn. SGAU*, 2011, vol. 27, no. 3, pp. 47–56.
13. Vedeneev, V.V., Kolotnikov, M.E., and Makarov, P.V., Experimental validation of numerical blade flutter prediction, *J. Propuls. Power*, 2015, vol. 31, pp. 1281–1291.
14. Kolotnikov, M.E., Makarov, P.V., and Sachin, V.M., Study of the dynamic intensity of a wide-chord fan during bench testing, *Aviats.-Kosm. Tekh. Tekhnol.*, 2008, vol. 56, no. 9, pp. 58–64.

*Translated by O. Lotova*